COMMUNICATION Selective Promotion of CO_2-to--Fuels Conversion by Tuning Catalyst Mesostructure

Selective Promotion of CO_2-to-Fuels Conversion by Tuning Catalyst Mesostructure.

Youngmin Yoon,[a] Anthony Shoji Hall,[a],[b] and Yogesh Surendranath*[a]

Abstract: An electrode's performance for CO_2-to-fuels catalysis is a complex convolution of surface structure and transport effects. Using well-defined mesostructured silver inverse opal (Ag-IO) electrodes, we demonstrate that mesostructure-induced transport limitations alone serve to *increase* the per-area turnover frequency for CO_2 activation while simultaneously improving reaction selectivity. The specific activity for CO evolution catalysis systematically *rises* by three-fold *and* the specific activity for H_2 evolution catalysis systematically *declines* by ten-fold with increasing mesostructural roughness of Ag-IOs. By exploiting the compounding influence of both of these effects, we demonstrate that mesostructure, rather than surface structure, can be used to tune CO evolution selectivity from < 5% to > 80%. These results establish electrode mesostructuring as a powerful complementary tool for tuning both the selectivity and efficiency of CO_2-to-fuels catalysis.

Intermittent renewable electricity can be stored in the energy dense bonds of chemical fuels via the electrochemical reduction of CO_2[1–4]. However, the low efficiencies and high costs of current CO_2-to-fuels technologies have impeded their widespread commercial deployment[4]. A principle impediment to the development of practical CO_2-to-fuels devices is the lack of efficient and selective catalysts for the multi-electron, multi-proton reduction of CO_2. CO_2 reduction is most practically carried out in aqueous electrolytes, in which the reduction of protons to H_2 often outcompetes CO_2-to-fuels conversion, eroding reaction selectivity. Thus, a key requirement for any viable catalyst is the ability to preferentially activate CO_2 over H^+ despite the relative kinetic difficulty of the former. The importance of this initial selectivity-determining step is highlighted on Ag and Au surfaces[3,5] which principally generate CO (eq. 1) and H_2 (eq. 2) via the following electrochemical half reactions:

$$CO_2 + 2H^+ + 2e^- \rightarrow CO + H_2O \quad \text{(eq. 1)}$$

$$2H^+ + 2e^- \rightarrow H_2 \quad \text{(eq. 2)}$$

While the CO produced via eq. 1 can be further reduced to a wide array of higher order carbonaceous products on Cu metal surfaces, the initial kinetic branching ratio between CO and H_2 production places an upper limit on overall CO_2-to-fuels selectivity[3,5–8]. Despite the central role of this initial kinetic branch point, there remains a scarcity of general materials design principles for realizing selective CO_2 over H^+ conversion, impeding the systematic development of CO_2-to-fuels catalysts[3].

As electrocatalysis is an interfacial phenomenon, the relative rates of CO_2 and H^+ activation will be dictated both by the intrinsic selectivity of surface active sites as well as the local concentration of reaction partners involved in the rate-controlling steps of each pathway. While the bulk concentration of all relevant chemical species can be easily measured and varied by changing, for example, the pH, buffer strength, or CO_2 partial pressure, the local concentration of these species at surface active sites is typically unknown and highly dependent on the micro and mesostructure of the electrode, which establishes complex diffusional gradients under steady-state catalysis conditions[3,9,10]. This is particularly true for CO_2-to-fuels catalysts because they are typically investigated in a CO_2/HCO_3^- electrolyte. This buffer displays very slow equilibration kinetics due to sluggish CO_2 hydration ($t_{1/2} \approx 19$ s)[11]. As a result, the local pH environment at the electrode surface is expected to be significantly more alkaline than the bulk environment[9]. Despite the potentially dramatic role of local diffusional gradients in determining the selectivity of CO_2-to-fuels conversion, there exist a paucity of methods for systematically varying the diffusional manifold of the electrode while holding other aspects of the catalyst surface (e.g. faceting, grain size, etc.) constant. Indeed, recent reports of highly efficient, selective CO evolving catalysts feature high surface area metal films prepared by methods such as nanoparticle deposition[12,13], de-alloying[14], or reduction of an oxide[6,15–18] or chloride precursor phase[19]. All of these preparation methods serve to simultaneously alter the surface structure and the micro/mesostructure of the electrode, making it difficult, if not impossible, to deconvolute the relative contributions of each to the observed electrode activity and selectivity.

For a simple electrochemical reaction involving a single diffusion species that converts to a single product, transport limitations at an electrode surface can only serve to decrease intrinsic catalytic performance. However, for aqueous CO_2-to-fuels catalysis in which multiple reaction partners are involved in multiple concurrent reaction paths, transport limitations can lead to several possible outcomes in terms of overall electrode performance. If the undesired pathway is more sensitive to transport limitations than the desired reaction, electrode selectivity will improve, but the specific activity for the desired reaction will remain unchanged. We have recently demonstrated this phenomenon for Au-catalyzed CO_2 reduction,[10] for which mesostructuring induces transport limitations that suppress the rate of H_2 evolution but leave the rate of CO production largely unchanged[10]. Likewise, enhanced selectivity on mesostructured oxide-derived Ag surfaces has been attributed, in part, to transport-limitation-induced H_2 suppression[18]. A tantalizing alternative possibility, which is entirely unprecedented, is one in which transport limitations serve to *promote* the desired reaction while *simultaneously suppressing* the undesired reaction. In this limit, the electrode's specific activity, selectivity, and geometric activity would all be enhanced concomitantly. Herein, we

[a] Y. Yoon, Prof. A. S. Hall, Prof. Y. Surendranath
Department of Chemistry
Massachusetts Institute of Technology
77 Massachusetts Ave., 18-163, Cambridge MA 02139, USA
E-mail: yogi@mit.edu
[b] Prof. A. S. Hall
Materials Science and Engineering Department
Johns Hopkins University
3400 North Charles Street, Baltimore, MD 21218, USA

Supporting information for this article is given via a link at the end of the document.

synthesize ordered mesostructured Ag-IO electrodes and demonstrate that increasing the thickness of the mesostructure, without changing the surface structure, effects simultaneous *promotion* of CO generation and *suppression* of HER, allowing for dramatic tuning of CO_2-to-fuels selectivity from <5 % to >80 %.

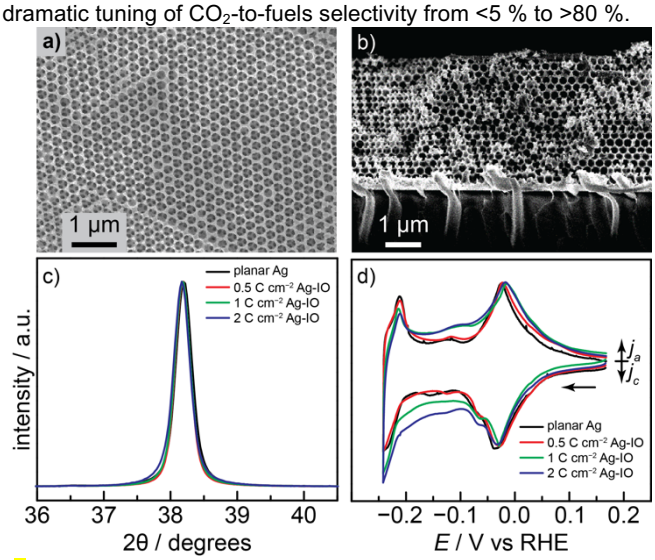

Figure 1. Top down (a) and cross-sectional (b) SEM micrographs of a Ag-IO film prepared by passing 1 C/cm^2 Ag deposition charge. Normalized X-ray diffraction peak for the $Ag_{(111)}$ reflection (c) and cyclic voltammograms (d) of thallium UPD and stripping, normalized to the −0.03 V peak, for Ag-IO samples prepared by passing 0.5 (red), 1 (green), and 2 (blue) C/cm^2 Ag deposition charge and nominally planar Ag films (black).

Ordered mesostructured Ag inverse opals (Ag-IO) exhibiting uniform surface structure, porosity, and tortuosity were prepared by the replication of colloidal polystyrene thin films on Au coated glass slides. The details of the 200 nm polystyrene sphere deposition, sintering, and silver electrodeposition can be found in the SI[20,21]. Ag was electrochemically deposited into the necked polystyrene opal using a commercial alkaline Ag plating solution containing Ag succinimide. By controlling the amount of Ag deposited, the thicknesses of the Ag-IO films were systematically altered. Following deposition, the polystyrene spheres were selectively removed by dissolution and extraction into toluene, leaving the bare Ag-IO with ordered porosity. Scanning electron microscope (SEM) images reveal the formation of smooth, ordered, porous Ag-IO networks with ~200 nm voids interconnected by ~50 nm channels (**Figure 1a, b**). The pores generally display a hexagonal closed packed arrangement, reflecting the FCC lattice of the polystyrene host template. The porosity remains uniform over the entire thickness of the film reflecting the fidelity of this synthetic method. By varying the Ag deposition charge passed from 0.5 to 2 C/cm^2 we are able to tune the thickness of the porous film from ~1.7 to ~6.2 μm (**Figure S1**). We determined the electrochemically active surface area (ECSA) of each electrode by dividing its double layer capacitance (DLC) by the 25 μF/cm^2 value for a planar Ag surface[22]. The capacitance current vs scan rate plots are linear, indicating negligible ion transport resistances within the Ag-IO film (**Figure S2**). These ECSA values were normalized to the geometric area of each electrode to determine its roughness factor (RF). By varying the Ag deposition charge, we are able to tune the RF from ~43 to ~110, corresponding to a ~4.5 μm span of Ag-IO thickness (**Figure S3**) Together these observations establish that electrodeposition into self-assembled opal templates generates tunable porous electrodes.

The grain and surface structure of the Ag-IO is invariant with film thickness. X-ray photoelectron spectroscopy (XPS) confirms the presence of a pure Ag metal surface free of any detectable metal impurities (**Figure S4**). Additionally, X-ray diffraction studies (**Figure 1c**) reveal the presence of polycrystalline Ag with an average grain size of 35 nm, which is similar across all Ag-IO thicknesses. Thallium underpotential deposition (UPD)[23] was used to characterize the population of Ag surface facets present in each Ag-IO. A broad thallium UPD wave is observed in the cyclic voltammogram at −0.03 V (all potentials are reported versus the reversible hydrogen electrode, RHE) with a pronounced shoulder at −0.07 V and a subsequent small UPD wave at −0.15 V (**Figure 1d**)[23]. All of these features are well separated from the bulk deposition wave that onsets at −0.20 V. The UPD data is consistent with a broad distribution of surface exposed Ag facets. Importantly, the same UPD features appear with similar relative magnitudes over a range of Ag-IO thicknesses as well as nominally planar films deposited in the absence of the IO template. Together the data indicate that the bulk and surface composition and structure of these Ag films are largely invariant across a wide range of electrode thicknesses and porosities.

To probe the dependence of CO_2-to-fuels selectivity on the mesostructure of the electrode, we compared the performance of a variety of Ag-IO samples of different thickness as well as nominally planar Ag films (RF = ~4) deposited in the absence of an IO host template. Data were collected as a function of potential from −0.50 V to −0.80 V in CO_2-saturated 0.1 M $KHCO_3$ (pH 6.8) (**Figure 2**). To effectively compare the data across both planar Ag films and Ag-IO films, the data are color coded by electrode RF. Planar Ag electrodes uniformly display very low selectivity for CO production over the entire range of the potentials explored (**Figure 2**), with the onset of measureable CO selectivity occurring beyond -0.75 V. In contrast, we observe significantly enhanced faradaic efficiency (FE) for CO production for Ag-IO samples along with a general increase in CO selectivity as the Ag-IO thicknesses and electrode RF values increase. Indeed, for the thickest Ag-IO samples examined (~6.2 μm), which display roughness factors of >100, we observed appreciable CO selectivity at -0.50 V which rises to >80% at -0.70 V. Together the data indicate that, remarkably, increasing the electrode roughness factor via mesostructuring is sufficient to enhance the CO FE from <5% to >80 %.

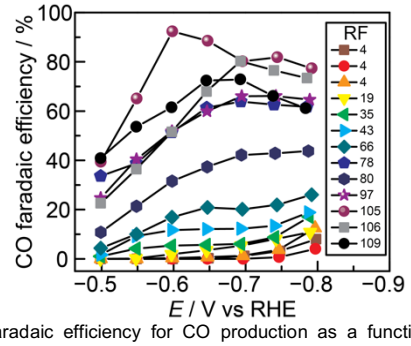

Figure 2. Faradaic efficiency for CO production as a function of applied potential for Ag films of varying RF. All data were collected in CO_2-saturated 0.1 M $KHCO_3$.

To probe the origin of the enhanced CO selectivity as a function of RF, we compared the specific activity for CO and H_2 production at a variety of potentials for Ag electrodes of varying porosities and thicknesses (**Figure 3**). Specific current densities (*j*) were obtained by normalizing the partial currents of H_2 and CO production to the ECSA of each electrode. In CO_2-saturated 0.1 $KHCO_3$ electrolyte, the low RF planar Ag electrodes display the highest specific activities for H_2 production over the entire potential range, whereas the thickest Ag-IO samples display the lowest j_{H2} values (**Figure 3a**). Indeed, at −0.8 V, the specific activity for H_2 production declines systematically as a function of electrode RF with an ~10 fold decline over the range of electrode RF values explored here (**Figure 3c**). These data are in line with our previous observations on Au-IO electrodes suggesting that H_2 suppression is a general phenomenon that arises intrinsically as a consequence of increased electrode mesostructure.

Remarkably, the suppression of H_2 production is not the only source of enhanced overall selectivity. In contrast to the behavior observed for H_2 production, the low RF Ag electrodes display the lowest specific activities for CO production over the entire potential range, whereas the thickest Ag-IO samples display the highest j_{CO} values (**Figure 3b**).. Indeed, at −0.8 V, the specific activity for CO production *rises* systematically as a function of electrode RF with a ~3 fold increase over the range of electrode RF values explored here (**Figure 3d**). Together the data indicate that there is a synergistic interplay between simultaneous promotion of CO evolution and suppression of H_2 evolution that together, give rise to the dramatic improvement in overall CO_2-to-fuels selectivity. These results demonstrate that electrode mesostructuring is a powerful strategy for tuning CO_2-to-fuels selectivity *and* activity, independent of the surface structure and/or active site density of the catalyst.

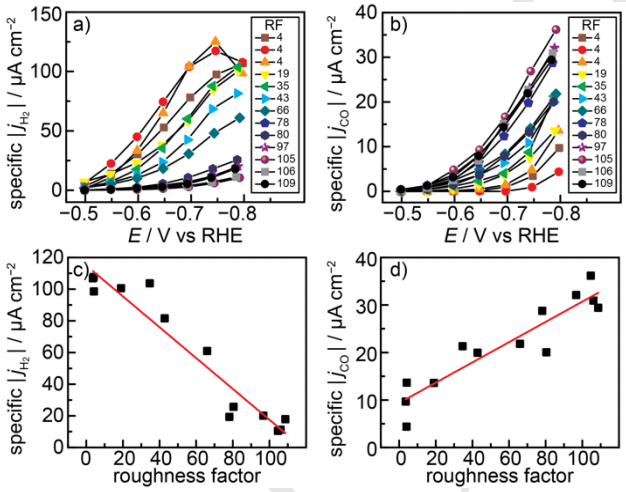

Figure 3. Specific current density for H_2 (a) and CO (b) evolution as a function of applied potential for Ag films of varying roughness factor (RF). Specific current density at −0.80 V for H_2 (c) and CO (d) evolution as a function of electrode RF. All data were collected in CO_2-saturated 0.1 M $KHCO_3$.

Whereas increasing the thickness and roughness of a Ag-IO serves to systematically amplify diffusional gradients at the catalyst surface, rotation of a planar Ag electrode achieves the opposite effect by inducing convective flow of electrolyte to the electrode. To amplify the diffusional gradients generated at the electrode surface, we conducted rotation rate dependent studies at a slightly more negative potential, −0.85 V, to induce a higher overall rate of catalysis. In line with the above results on Au-IO films, increasing the rotation rate of a polished polycrystalline Ag cone electrode serves to systematically increase the rate of H_2 production (**Figure 4a**). We observe that the specific activity for H_2 production *rises* by ~40% by increasing the rotation rate from 700 to 3500 rpm. These results are similar to the behavior observed for Au-catalyzed H_2 production which is also enhanced with increasing rotation rate[10]. Mechanistic studies of Au electrodes indicate that the rate of H_2 evolution catalysis is highly sensitive to the local pH and buffer composition of the electrolyte that establish the proton donor environment at the electrode surface[24]. Thus, we postulate that the systematic suppression in H_2 evolution observed upon increasing electrode RF or decreasing rotation rate also results from an elevated local pH that serves to deplete the local concentration of proton donors at the surface.

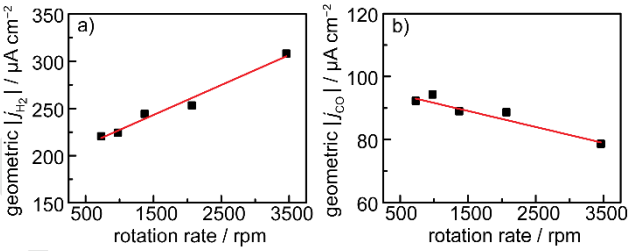

Figure 4. Geometric current density at −0.85 V for H_2 (a) and CO (b) evolution as a function of rotation rate for a Ag rotating cone electrode polarized in CO_2-saturated 0.1 M $KHCO_3$. Red lines serve as guides to the eye.

Increasing the rotation rate has the opposite effect on the rate of CO production. The specific activity for CO production *declines* by ~15% upon increasing the rotation rate from 700 to 3500 rpm (**Figure 4b**). This observation is very unusual in heterogeneous electrocatalysis because it implies that *accelerated* mass transport serves, counter-intuitively, to *impede* the rate of CO production under these conditions. These results are also in contrast to observations on Au electrodes, for which the rate of CO production is largely independent of the electrode rotation rate[10,24]. Detailed mechanistic studies of Au-catalyzed CO production establish that CO_2 activation proceeds via rate limiting single electron transfer and adsorption of CO_2 rather than concerted electron-proton transfer[24], making the reaction largely insensitive to the changes in the local proton donor environment. While an analogous mechanistic understanding of the *activation-controlled* kinetics of Ag-catalyzed CO production under these conditions does not exist and is the subject of ongoing investigations, we note that a strong dependence of CO production on the proton donor concentrations would give rise to the opposite of the effect observed here – systematic inhibition of CO production with increased RF. While we cannot rule out several competing effects,[25] we note that the local activity of K^+ and CO_3^{2-} must rise in tandem with elevated local pH and that these species may serve to promote CO production in this system[26–29]. Irrespective of the specific mechanism of promotion, these results highlight that electrode mesostructuring is a powerful tool for promoting the specific activity of the surface for CO_2-to-fuels catalysis.

By synthesizing a series of ordered mesostructured Ag electrodes, we have demonstrated that catalyst mesostructure

induces *both* a dramatic *suppression* in the rate of the undesirable H_2 evolution reaction as well as a significant *promotion* in the rate of the desired CO_2-to-fuels reaction. As a result, we have shown that mesostructuring is in and of itself sufficient to tune the selectivity of CO_2-to-fuels catalysts from <5% to >80%. As any practical CO_2-to-fuels electrode must consist of a high degree of porosity, this work highlights that the local diffusional gradients that develop within these pores play a key role in defining CO_2-to-fuels conversion efficiency and selectivity. The work introduces electrode mesostructuring as powerful complementary strategy for promoting selective, efficient CO_2-to-fuels catalysis.

Acknowledgements

We thank Anna Wuttig and Bing Yan for helpful discussions. This research was supported by the Air Force Office of Scientific Research under award FA9550-15-1-0135 and by the MIT Department of Chemistry through junior faculty funds for Y.S. This work made use of Shared Experimental Facilities supported in part by the MRSEC Program of the National Science Foundation under award number DMR–1419807.

Keywords: CO_2 reduction • electrocatalysis • mesoporous materials • mass transport • renewable energy

[1] W. Tang, A. A. Peterson, A. S. Varela, Z. P. Jovanov, L. Bech, W. J. Durand, S. Dahl, J. K. Nørskov, I. Chorkendorff, *Phys. Chem. Chem. Phys.* **2012**, *14*, 76–81.

[2] K. P. Kuhl, T. Hatsukade, E. R. Cave, D. N. Abram, J. Kibsgaard, T. F. Jaramillo, *J. Am. Chem. Soc.* **2014**, *136*, 14107–14113.

[3] Y. Hori, in *Mod. Asp. Electrochem.* (Eds.: C. Vayenas, R. White, M. Gamboa-Aldeco), Springer New York, New York, NY, **2008**, pp. 89–189.

[4] J.-P. Jones, G. K. S. Prakash, G. A. Olah, *Isr. J. Chem.* **2014**, *54*, 1451–1466.

[5] A. A. Peterson, J. K. Nørskov, *J. Phys. Chem. Lett.* **2012**, *3*, 251–258.

[6] C. W. Li, M. W. Kanan, *J. Am. Chem. Soc.* **2012**, *134*, 7231–7234.

[7] M. Gattrell, N. Gupta, A. Co, *J. Electroanal. Chem.* **2006**, *594*, 1–19.

[8] K. P. Kuhl, E. R. Cave, D. N. Abram, T. F. Jaramillo, *Energy Environ. Sci.* **2012**, *5*, 7050.

[9] N. Gupta, M. Gattrell, B. MacDougall, *J. Appl. Electrochem.* **2006**, *36*, 161–172.

[10] A. S. Hall, Y. Yoon, A. Wuttig, Y. Surendranath, *J. Am. Chem. Soc.* **2015**, *137*, 14834–14837.

[11] Y. Pocker, D. W. Bjorkquist, *J. Am. Chem. Soc.* **1977**, *99*, 6537–6543.

[12] D. Kim, J. Resasco, Y. Yu, A. M. Asiri, P. Yang, *Nat. Commun.* **2014**, *5*, 4948.

[13] C. Kim, H. S. Jeon, T. Eom, M. S. Jee, H. Kim, C. M. Friend, B. K. Min, Y. J. Hwang, *J. Am. Chem. Soc.* **2015**, *137*, 13844–13850.

[14] Q. Lu, J. Rosen, Y. Zhou, G. S. Hutchings, Y. C. Kimmel, J. G. Chen, F. Jiao, *Nat. Commun.* **2014**, *5*, 3242.

[15] Y. Chen, C. W. Li, M. W. Kanan, *J. Am. Chem. Soc.* **2012**, *134*, 19969–19972.

[16] L. Q. Zhou, C. Ling, M. Jones, H. Jia, *Chem. Commun.* **2015**, *51*, 17704–17707.

[17] R. Kas, K. K. Hummadi, R. Kortlever, P. de Wit, A. Milbrat, M. W. J. Luiten-Olieman, N. E. Benes, M. T. M. Koper, G. Mul, *Nat. Commun.* **2016**, *7*, 10748.

[18] M. Ma, B. J. Trześniewski, J. Xie, W. A. Smith, *Angew. Chemie Int. Ed.* **2016**, 9748–9752.

[19] Y.-C. Hsieh, S. D. Senanayake, Y. Zhang, W. Xu, D. E. Polyansky, *ACS Catal.* **2015**, *5*, 5349–5356.

[20] R. G. Shimmin, A. J. DiMauro, P. V. Braun, *Langmuir* **2006**, *22*, 6507–6513.

[21] D. Hung, Z. Liu, N. Shah, Y. Hao, P. C. Searson, *J. Phys. Chem. C* **2007**, *111*, 3308–3313.

[22] A. J. Motheo, S. A. S. Machado, M. H. Van Kampen, J. R. Santos Jr., *J. Braz. Chem. Soc.* **1993**, *4*, 122–127.

[23] A. Bewick, B. Thomas, *J. Electroanal. Chem. Interfacial Electrochem.* **1977**, *84*, 127–140.

[24] A. Wuttig, M. Yaguchi, K. Motobayashi, M. Osawa, Y. Surendranath, *Proc. Natl. Acad. Sci.* **2016**, *113*, E4585–E4593.

[25] J. Rosen, G. S. Hutchings, Q. Lu, S. Rivera, Y. Zhou, D. G. Vlachos, F. Jiao, *ACS Catal.* **2015**, *5*, 4293–4299.

[26] D. Strmcnik, M. Uchimura, C. Wang, R. Subbaraman, N. Danilovic, D. van der Vliet, A. P. Paulikas, V. R. Stamenkovic, N. M. Markovic, *Nat. Chem.* **2013**, *5*, 300–306.

[27] Y. J. Tong, *Chem. Soc. Rev.* **2012**, *41*, 8195.

[28] S. Verma, X. Lu, S. Ma, R. I. Masel, P. J. A. Kenis, *Phys. Chem. Chem. Phys.* **2016**, *18*, 7075–7084.

[29] M. R. Thorson, K. I. Siil, P. J. a. Kenis, *J. Electrochem. Soc.* **2012**, *160*, F69–F74.

Entry for the Table of Contents

COMMUNICATION

Mesostructuring Ag catalysts leads to an unprecedented promotion of CO_2-to-fuels catalysis and a simultaneous suppression of H_2 evolution. This results in a dramatic tunability in CO production selectivity from <5% to >80% simply by increasing mesostructured film thickness.

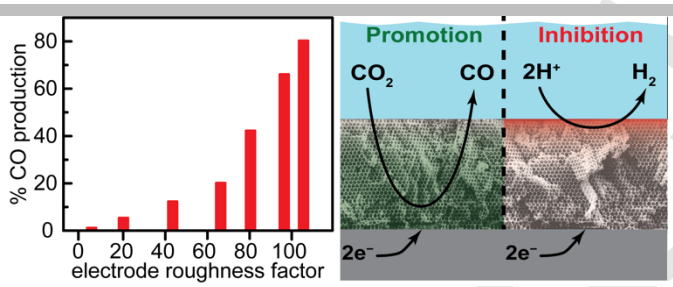

*Y. Yoon, A. S. Hall, Y. Surendranath**

Page No. – Page No.

Selective Promotion of CO_2-to-Fuels Conversion by Tuning Catalyst Mesostructure.